Gastroenterology 2016;150:591–598

Development and Validation of a Classification System to Identify High-Grade Dysplasia and Esophageal Adenocarcinoma in Barrett's Esophagus Using Narrow-Band Imaging

Prateek Sharma,[1] Jacques J. G. H. M. Bergman,[2] Kenichi Goda,[3] Mototsugu Kato,[4] Helmut Messmann,[5] Benjamin R. Alsop,[1] Neil Gupta,[6] Prashanth Vennalaganti,[1] Matt Hall,[1] Vani Konda,[7] Ann Koons,[7] Olga Penner,[5] John R. Goldblum,[8] and Irving Waxman[7]

[1]Department of Gastroenterology and Hepatology, Veterans Affairs Medical Center and University of Kansas School of Medicine, Kansas City, Missouri; [2]Department of Gastroenterology and Hepatology, Academic Medical Center, Amsterdam, The Netherlands; [3]Department of Endoscopy, The Jikei University School of Medicine, Tokyo, Japan; [4]Division of Endoscopy, Hokkaido University Hospital, Sapporo, Japan; [5]Department of Internal Medicine, Clinic Augsburg, Augsburg, Germany; [6]Department of Gastroenterology, Loyola University Medical Center, Maywood, Illinois; [7]Center for Endoscopic Research and Therapeutics (CERT), The University of Chicago Medicine, Chicago, Illinois; and [8]Department of Anatomic Pathology, Cleveland Clinic Foundation, Cleveland, Ohio

BACKGROUND & AIMS: Although several classification systems have been proposed for characterization of Barrett's esophagus (BE) surface patterns based on narrow-band imaging (NBI), none have been widely accepted. The Barrett's International NBI Group (BING) aimed to develop and validate an NBI classification system for identification of dysplasia and cancer in patients with BE. **METHODS:** The BING working group, composed of NBI experts from the United States, Europe, and Japan, met to develop a validated, consensus-driven NBI classification system for identifying dysplasia and cancer in BE. The group reviewed 60 NBI images of nondysplastic BE, high-grade dysplasia, and esophageal adenocarcinoma to characterize mucosal and vascular patterns visible by NBI; these features were used to develop the BING criteria. We then recruited adult patients undergoing surveillance or endoscopic treatment for BE at 4 institutions in the United States and Europe, obtaining high-quality NBI images and performing histologic analysis of biopsies. Experts individually reviewed 50 NBI images to validate the BING criteria, and then evaluated 120 additional NBI images (not previously viewed) to determine whether the criteria accurately predicted the histology results. **RESULTS:** The BING criteria identified patients with dysplasia with 85% overall accuracy, 80% sensitivity, 88% specificity, 81% positive predictive value, and 88% negative predictive value. When dysplasia was identified with a high level of confidence, these values were 92%, 91%, 93%, 89%, and 95%, respectively. The overall strength of inter-observer agreement was substantial ($\kappa = 0.681$). **CONCLUSIONS:** The BING working group developed a simple, internally validated system to identify dysplasia and EAC in patients with BE based on NBI results. When images are assessed with a high degree of confidence, the system can classify BE with >90% accuracy and a high level of inter-observer agreement.

Keywords: NDBE; Esophageal Cancer; Risk Factors; Endoscopy.

Barrett's esophagus (BE) is a precursor for esophageal adenocarcinoma (EAC), the most rapidly increasing cancer in the Western world.[1–5] BE is suspected when intestinal-type columnar metaplasia extends beyond the gastroesophageal junction into the esophagus.[6,7] Although controversial, endoscopic surveillance is generally recommended in patients with a confirmed diagnosis of BE, with the aim of detecting dysplasia/EAC in an early, curable stage.[6] Current surveillance guidelines for BE also recommend random biopsy sampling of Barrett's epithelium to identify areas of suspected dysplasia.[8] The Seattle protocol calls for random 4-quadrant biopsy specimens to be obtained at intervals of every 1 to 2 cm for the entire length of BE.[8–10]

Despite rigorous BE surveillance procedures, early cancer can go undetected because of inherent limitations in various aspects of the surveillance protocol.[6] Dysplasia in BE can be patchy and focal in nature, and several studies have shown that standard white light endoscopy (WLE) might not reliably reveal early neoplasia in BE.[9,11,12] Furthermore, the irregular extent and severity of dysplasia in Barrett's epithelium increases the chances that early cancer may not be detected with random biopsies. It has been reported that random biopsies obtained with WLE might sample only 4% to 5% of Barrett's epithelium.[9,11]

To overcome some of the deficiencies associated with BE surveillance, a number of alternative endoscopic techniques have been proposed to enhance the detection of dysplasia in BE.[6] Narrow band imaging (NBI), high-resolution endoscopy, chromoendoscopy, autofluorescence imaging, and confocal endomicroscopy have been evaluated for their potential to improve the detection of dysplasia in BE.[6] These advanced imaging tools not only have the potential to

Abbreviations used in this paper: BE, Barrett's esophagus; BING, Barrett's International NBI Group; EAC, esophageal adenocarcinoma; HGD, high-grade dysplasia; NBI, narrow-band imaging; NDBE, nondysplastic Barrett's esophagus; WLE, white light endoscopy.

Most current article

0016-5085/$36.00
http://dx.doi.org/10.1053/j.gastro.2015.11.037

CLINICAL AT

improve endoscopic detection of early neoplasia in BE, but also may reduce the cost, procedure time, and sampling error associated with multiple random esophageal biopsies.[6,12–14]

NBI is one of the most widely studied tools for the detection and characterization of early neoplasia in patients undergoing surveillance for BE.[15–17] Using NBI, several groups have described specific mucosal and vascular patterns characteristic of Barrett's epithelium.[18–24] However, despite promising initial findings, subsequent validation studies of these NBI classification systems have reported disappointing results.[25–29] Additionally, the proposed criteria are complex and diverse, limiting their use in daily clinical practice.

Despite the importance of accurate characterization of dysplasia in BE, there is currently no authoritative guidance on how this should be done using NBI. Although previous attempts at NBI classification systems have been made, these have been based on single-center studies, which are not internally validated, with limited numbers of patients and limited reproducibility of results.[18–20,24] With these points in mind, we convened an international working group, the Barrett's International NBI Group (BING), to develop and validate a prospective, consensus-driven NBI classification system that can be used to predict the presence or absence of dysplasia in BE.

Methods

Working Group and Development of Consensus-Driven Classification System

An international working group composed of 6 experts from the United States, Europe, and Japan (University of Kansas School of Medicine and Veterans Affairs Medical Center; The University of Chicago Medicine; Academic Medical Center, Amsterdam; the University of Augsburg, Germany; Hokkaido University, Japan; and The Jikei University School of Medicine, Japan) was convened to develop criteria for the use of NBI in the prediction of histopathology in BE. Members of the working group included gastroenterologists and endoscopists who were experts in BE and the use of NBI. The group initially met during the 2013 Digestive Disease Week meeting in Orlando, Florida. The entire process of creating, evaluating, and testing of the classification system was conducted in several phases.

In phase 1 of the study, the working group evaluated 60 high-quality NBI images of intestinal metaplasia/nondysplastic Barrett's esophagus (NDBE) and high-grade dysplasia (HGD)/esophageal adenocarcinoma (EAC) provided by centers from the United States and Europe (University of Kansas School of Medicine; The University of Chicago Medicine; Academic Medical Center; and the University of Regensburg) to develop a classification system based on the mucosal and vascular patterns observed in the Barrett's epithelium. Mucosal and vascular patterns in each NBI image were classified as "regular" or "irregular" based on characteristics agreed upon by the working group (Table 1). Regular mucosal patterns were marked by circular, ridged/villous, or tubular patterns, and irregular mucosa was marked by absent or irregular surface patterns (Figures 1*A–F* and 2*A–F*). Regular vascular patterns were defined by blood vessels situated regularly along or between mucosal ridges and/or those showing normal, long, branching patterns; irregular vascular patterns were marked by focally or diffusely distributed vessels not following the normal architecture of the mucosa (Figures 1*A–F* and 2*A–F*). Images not readily identified as regular or irregular were deemed "uncertain." Consensus was achieved among all experts regarding this classification system.

Table 1. Consensus-Driven NBI Classification of Barrett's Epithelium

Morphologic characteristics	Classification
Mucosal pattern	
Circular, ridged/villous, or tubular patterns	Regular
Absent or irregular patterns	Irregular
Vascular pattern	
Blood vessels situated regularly along or between mucosal ridges and/or those showing normal, long, branching patterns	Regular
Focally or diffusely distributed vessels not following normal architecture of the mucosa	Irregular

Endoscopic Procedures and Narrow-Band Imaging System

In phase 2 of the study, NBI images for this multicenter, prospective, study were captured from adult patients undergoing surveillance or endoscopic treatment for BE at 4 institutions in the United States and Europe after respective permissions from the Institution Review Boards of each institution. Patients included in the study were required to be able to tolerate oral proton pump inhibitors and to discontinue the use of aspirin, nonsteroidal anti-inflammatory drugs, or clopidogrel 7 days before and after all endoscopic ablation procedures. Patients were excluded from the study if they met any of the following criteria: were pregnant or were planning a pregnancy; had esophageal strictures preventing the passage of an endoscope; had active erosive esophagitis; had received prior endoscopic therapy (eg, endoscopic mucosal resection, radiofrequency ablation); had received prior esophageal radiation therapy; had a history of esophageal varices or coagulopathy; or had evidence of esophageal varices during therapeutic endoscopy.

Individuals who met eligibility criteria and provided informed consent underwent routine upper endoscopy with a high-definition NBI endoscope (GIF-HQ190 [dual focus]; Olympus Inc., Tokyo, Japan) performed by 1 of 4 expert endoscopists (University of Kansas School of Medicine; The University of Chicago Medicine; Academic Medical Center; University of Regensburg). The narrow-band optical filters (415 ± 20 nm, 445 ± 20 nm, and 500 ± 20 nm bands) used in NBI endoscopy, in contrast to the full-spectrum white light used in WLE, produce high-resolution, high-contrast images of mucosal and vascular patterns in Barrett's epithelium.[15–18]

A detailed endoscopic examination of BE was performed in all patients in the study. For each patient, Barrett's epithelium was carefully examined with the endoscope in overview mode (ie, in the center of the esophageal lumen), and then in close proximity to the BE surface (ie, approximately 3–5 mm away from the mucosa) using the "near focus" mode. In each of these

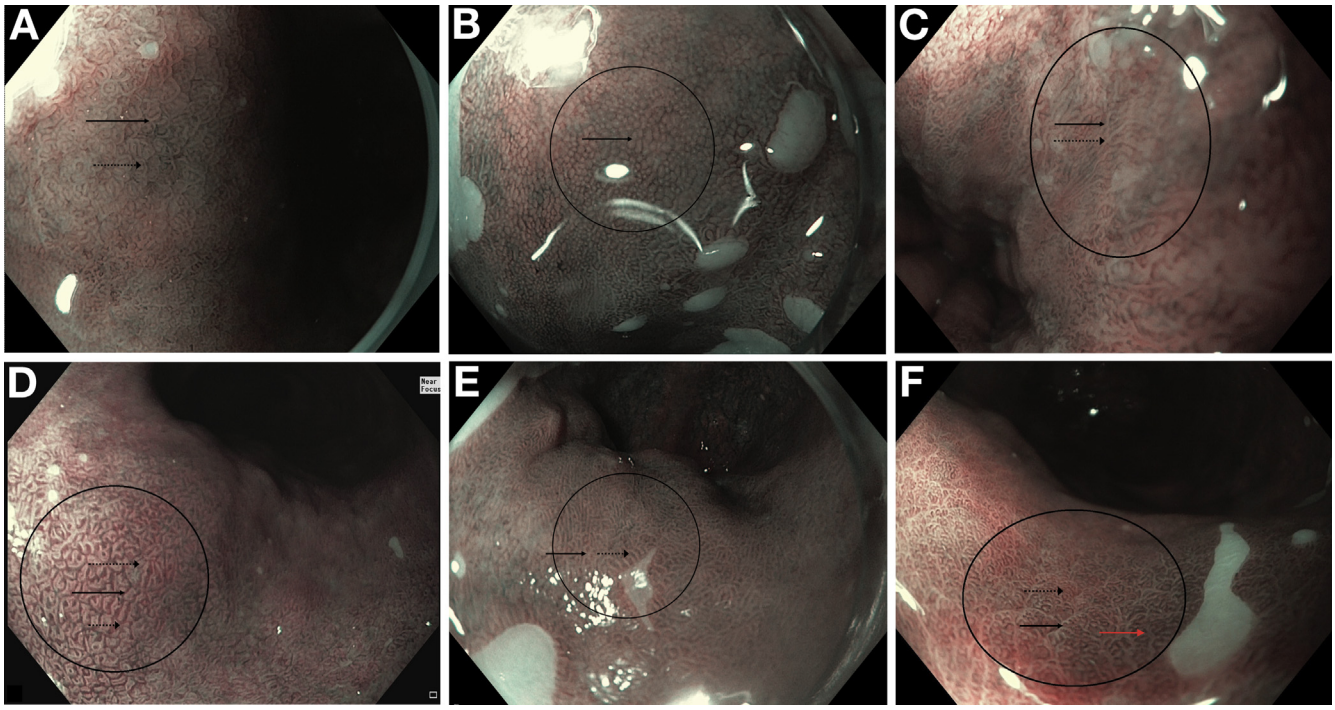

Figure 1. (*A*) High-resolution images of NDBE using NBI. Note the presence of circular mucosal patterns (*solid arrow*) that are arranged in an orderly fashion and blood vessels that clearly follow the mucosal architecture (*dashed arrows*). (*B*) High-resolution images of NDBE using NBI. Note the presence of circular mucosal patterns that are arranged in an orderly fashion and blood vessels that clearly follow the normal architecture of mucosa (*solid arrow*). (*C*) High-resolution images of NDBE using NBI. Note the presence of circular mucosal patterns (*solid arrow*) that are arranged in an orderly fashion and blood vessels that clearly follow the architecture of the mucosal ridges (*dashed arrows*). (*D*) High-resolution images of NDBE using NBI. Note the presence of ridge/villous mucosal patterns (*solid arrow*) that are arranged in an orderly fashion and blood vessels that are arranged in a regular fashion between the mucosal ridges (*dashed arrows*). (*E*) High-resolution images of NDBE using NBI. Note the presence of circular mucosal patterns (*solid arrow*) that are arranged in an orderly fashion and blood vessels that follow the architecture of the mucosa (*dashed arrows*). (*F*) High-resolution images of NDBE using NBI. Note the presence of circular (*solid black arrow*) and ridge/villous (*red arrow*) mucosal patterns arranged in an orderly fashion and blood vessels that follow the mucosal ridge architecture (*dashed arrows*).

positions, 4 to 5 high-quality images of areas representative of the different mucosal and vascular patterns defined by the working group (see Table 1) were captured, initially using WLE and then using NBI. No more than 4 images representing each of the 4 mucosal and vascular NBI classifications (see Table 1) within a given patient were used in the study (ie, 1 image per area of corresponding NBI-targeted biopsy). All images were stored in the high-quality TIFF format. NBI images of visible lesions ($\geq$10 mm), such as ulcers, nodules, or plaques, were excluded from the analysis.

For each NBI image captured for the study, corresponding target biopsies were obtained. Specimens were stored in separate containers for histopathologic examination and interpreted by a local pathologist. Subsequently, specimens were sent to a central experienced gastrointestinal pathologist (JG, Cleveland Clinic Foundation) for evaluation. For the purposes of this study, the report from the central pathologist was considered the gold standard. Specimens were graded as NDBE, low-grade dysplasia (LGD), indefinite for dysplasia (IND), or HGD/EAC.

Validation Studies

In phase 3 of the project, experts from the working group completed a web-based pretest designed to validate the newly defined consensus-driven NBI classification system. In this internal validation study, 50 NBI images (not previously viewed) were reviewed and classified as regular or irregular according to the definitions agreed upon in the working group meetings. Experts were blinded to the medical history of the patients and the corresponding pathology of the images used in the pretest. The images were selected from the databank of the 170 NBI images (that had corresponding histology reviewed by central pathologist) that were obtained during phase 2 of the project. These images were selected by investigators (BA, PV, NG) that were not involved in the assessment of the classification system.

This consensus-driven NBI classification system was used to predict the presence or absence of dysplasia in BE. Histology was predicted as NDBE or HGD/EAC based on each expert's classification of mucosal and vascular patterns in Barrett's epithelium as regular or irregular. The results of this validation pretest were discussed by the group during a face-to-face meeting during Digestive Disease Week 2014 (Chicago, Illinois).

In the final part of the study (phase 4), experts from the working group were asked to predict the histopathology of 120 NBI images not previously viewed in the pretest. This second web-based survey was designed to validate the ability of the consensus-driven NBI classification criteria to predict dysplasia in BE. Experts rated images as NDBE or HGD/EAC based on

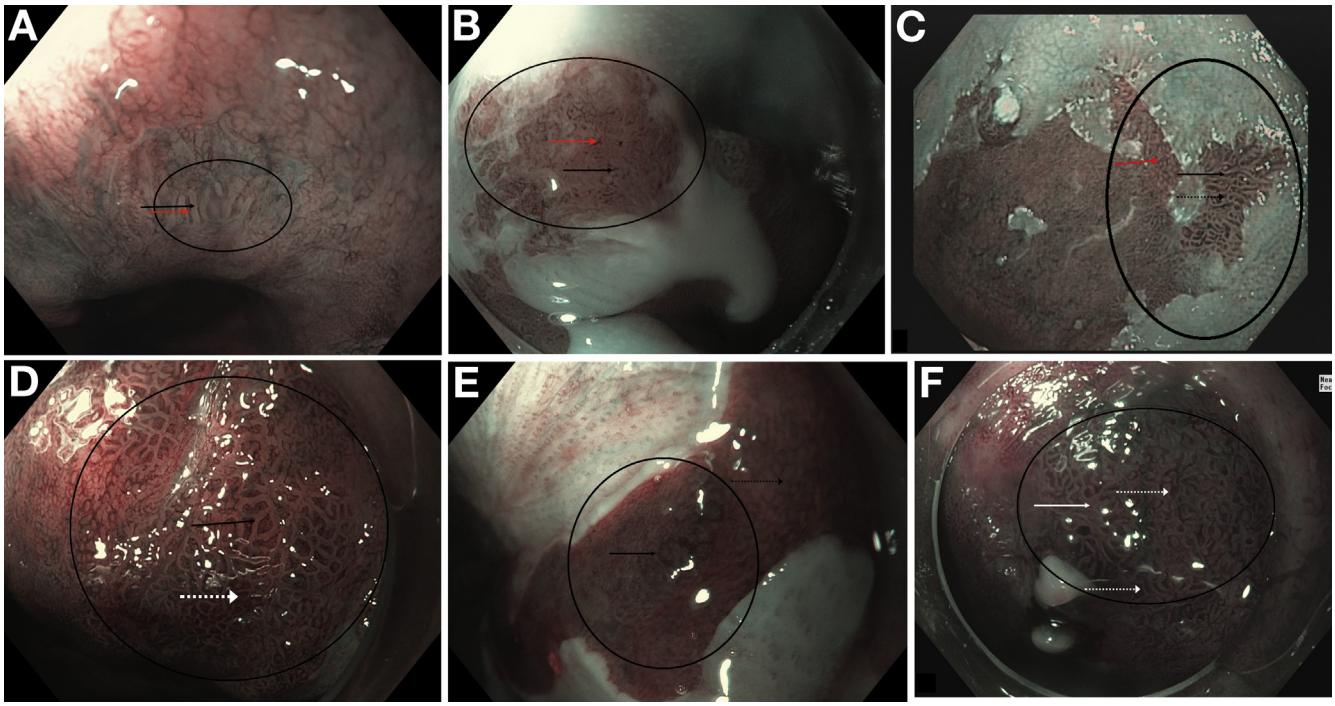

Figure 2. (*A*) High-resolution images of dysplastic BE using NBI. Irregular mucosal and vascular patterns in BE patient using NBI. Note the irregular mucosal (*black arrow*) and vascular patterns (*red arrow*). (*B*) High-resolution images of dysplastic BE using NBI. Irregular mucosal and vascular patterns in BE patient using NBI. Note the irregular mucosal (*black arrow*) and vascular patterns (*red arrow*). The vessels do not follow the normal architecture of the mucosa. (*C*) High-resolution images of dysplastic BE using NBI. Irregular mucosal and vascular patterns in BE patient using NBI. Note the irregular mucosal (*solid black arrow*) and vascular patterns (*dashed arrows*). In contrast, *red arrow* shows area on the mucosa where vessels are arranged in a regular fashion that follows the normal architecture of the mucosa. (*D*) High-resolution images of dysplastic BE using NBI. Irregular mucosal and vascular patterns in BE patient using NBI. Note the irregular mucosal and vascular patterns (*dashed arrows*). The focally or diffusely distributed vessels do not follow the normal architecture of the mucosa. (*E*) High-resolution images of dysplastic BE using NBI. Irregular mucosal and vascular patterns in BE patient using NBI. Note the irregular mucosal and vascular patterns (*solid arrow*) and in the *dashed arrows* in contrast shows regularly arranged mucosal and vascular pattern. (*F*) High-resolution images of dysplastic BE using NBI. Irregular mucosal and vascular patterns in BE patient using NBI. Note the irregular mucosal (*solid arrow*) and vascular patterns (*dashed arrows*).

their assessment of the mucosal and vascular patterns in the images. They also rated their level of confidence in their predictions as high or low, and they rated the quality of the images using a 5-point visual analog scale (1 = poor; 5 = excellent). Images were classified as uncertain if they could not be classified definitively as regular or irregular. Similar to the process in phase 3, the images for this phase were also selected by investigators (BA, PV, NG) that were not involved in the assessment of the classification system.

Sample Size Estimation and Statistical Analysis

Four studies have evaluated the accuracy of NBI in the prediction of dysplasia in BE.[26,27,30,31] Mean accuracy based on these studies was estimated at 77.5%. To determine if the mean accuracy could be improved by 4.0% using the new consensus-driven NBI classification system, 120 images with 6 reviewers would be required to achieve a power of >80% (assuming a one-sided α of 0.05). Although the majority of patients with BE have NDBE, a heterogeneous mix of dysplasia was necessary to obtain unbiased accuracy rates and inter-observer agreement in the current study; at least 20%−25% (60 images) of the images should be those of HGD or EAC.

Statistical analyses were performed using SAS software (version 9.4, SAS Institute, Cary, NC). Categorical variables were summarized using frequencies and percentages, and quantitative variable were summarized using means and SDs. Inter-observer agreement was calculated using κ-statistics and their 95% confidence intervals. A modified Likert scale developed by Landis and Koch[32] was used to interpret κ values (<.20 = poor; 0.21−.40 = fair; 0.41−.60 = moderate; 0.61−.80 = substantial; 0.81−1.00 = very good).

Accuracy rates for the ability of the NBI classification criteria to predict BE dysplasia were calculated for each expert reviewer, as well as for the overall group. Accuracy rates were stratified according to the experts' level of confidence in their predictions (high or low) and image quality (5-point visual analog scale). Sensitivity, specificity, positive predictive value, and negative predictive value were calculated for each variable using a 2 × 2 table analysis.

Student *t* test was used for quantitative variables to test the difference between study groups. Continuous variables with a non-normal distribution were compared using the Wilcoxon rank-sum test. Comparisons between categorical variables, such as accuracy rates, were performed using Fisher's exact test. All analyses assumed an α of 0.05 as the level of statistical significance.

Table 2. NBI Classification of Mucosal and Vascular Patterns in the Web-Based Pretest

	Regular, n (%)	Irregular, n (%)	Uncertain, n (%)
Mucosal pattern	169 (56.3)	92 (30.7)	39 (13.0)
Vascular pattern	171 (57.0)	99 (33.0)	30 (10.0)

Results

Patient Characteristics

Ninety-seven adult patients undergoing surveillance or endoscopic treatment for BE were eligible to be included in the study. The patients' mean age was 65.7 years (range, 40−85 years), 95.9% were male and 97.9% were white. Using the Prague criteria, the mean circumferential extent of BE was 3.1 cm (range, 0−13 cm) and the mean maximal extent was 5.2 (range, 1−15 cm). The majority of the patients (n = 82; 84.5%) had a hiatal hernia (mean size, 2.8 cm).

Development of the Barrett's International NBI Group Criteria (Phase 1)

During the initial working group meeting, the 6 experts reviewed 60 NBI images representative of different mucosal and vascular surface patterns in Barrett's epithelium. After detailed discussions regarding the archetypical characteristics of mucosal and vascular surface patterns in BE, the experts decided on 2 consensus-driven classifications for mucosal and vascular surface patterns: regular and irregular. The experts agreed that regular mucosal and vascular patterns could be used to predict NDBE, whereas irregular patterns were predictive of HGD/EAC. This new consensus-driven NBI classification system was named the BING Criteria.

Prospective Collection of Narrow-Band Imaging Images (Phase 2)

A total of 170 NBI images were prospectively obtained by 4 endoscopists who performed the procedures in this study. Of these, 50 were used in the web-based pretest, and 120 were used in the web-based final survey. The pathology (as rated by the central expert gastrointestinal pathologist) and quality (as rated on a 5-point visual analog scale by the experts in the working group) of the images included in the study are as follows. Among the images used in the pretest, 38 (75%) and 12 (24%) were NDBE and HGD/EAC, respectively. In the final survey, 75 (63%) and 45 (37%) were NDBE and HGD/EAC, respectively. Among the images with HGD/EAC, 25 of 45 were HGD (55.6%, or 20.8% of the total) and 20 of 45 were EAC (44.4%, or 16.7% of the total). Median score for image quality in both the pretest and final test was 4.

Internal Validation of the Barrett's International NBI Group Criteria and Pretest (Phase 3)

To internally validate the use of the BING Criteria in the classification of NBI surface patterns, the 6 experts completed a web-based pretest composed of 50 NBI images (pretest). Experts rated each image as regular, irregular, or uncertain based on the definitions agreed upon in the working group meetings (Table 2). Overall inter-observer agreement of the BING Criteria in the classification of mucosal and vascular patterns was moderate ($\kappa = 0.52$; 95% confidence interval: 0.48−0.56 and $\kappa = 0.48$; 95% confidence interval: 0.44-0.52) respectively.

Accuracy for Prediction of Dysplasia and Inter-Observer Agreement (Phase 4)

In a final web-based survey of the experts, the BING criteria were validated for their ability to predict dysplasia in BE. Experts from the working group reviewed 120 NBI images not previously viewed in the pretest and predicted histopathology using the BING criteria. Pathology was predicted as NDBE or HGD/EAC based on the experts' classification of mucosal and vascular patterns. The experts rated their level of confidence in their predictions as high or low. Experts were able to predict dysplasia with a high level of confidence in a total of 450 (62.5%) NBI images in the final survey (Table 3).

Table 4 illustrates the overall accuracy, sensitivity, specificity, negative predictive value, and positive predictive value of the BING Criteria for the prediction of dysplasia in BE (85%, 80%, 88%, 88%, and 81%, respectively). When predictions were made with a high level of confidence, there was a significant improvement in all parameters: 92%, 91%, 93%, 95%, and 89%, respectively. The impact of uncertain diagnosis was also evaluated. Of the total 720 images evaluated (120 by each of 6 reviewers), only 8.3% of vascular patterns were uncertain, 5% of mucosal patterns were uncertain, and in only 3.3% of images were both mucosal and vascular patterns uncertain. In cases of a single uncertain pattern, reviewers had low confidence in their ultimate histologic prediction 66.6% of the time. If both

Table 3. Experts' Confidence in Predictions of Dysplasia in NBI Images of Barrett's Esophagus

Prediction	Expert 1, n (%)	Expert 2, n (%)	Expert 3, n (%)	Expert 4, n (%)	Expert 5, n (%)	Expert 6, n (%)	Overall, n (%)
High-confidence	83 (69.2)	89 (74.2)	81 (67.5)	46 (38.3)	80 (66.7)	71 (59.2)	450 (62.5)
Low-confidence	37 (30.8)	31 (25.8)	39 (32.5)	74 (61.7)	40 (33.3)	49 (40.8)	270 (37.5)

Table 4. Accuracy and Sensitivity Analysis of the BING Criteria for the Prediction of Dysplasia in Barrett's Esophagus

Predictions	Accuracy, % (95% CI)	Sensitivity, % (95% CI)	Specificity, % (95% CI)	PPV, % (95% CI)	NPV, % (95% CI)
Overall	85.4 (82.6–87.9)	80.4 (75.6–85.1)	88.4 (85.4–91.4)	80.7 (75.9–85.4)	88.3 (85.2–91.2)
High-confidence	92.2 (89.3–94.5)	91.1 (86.8–95.4)	92.9 (89.8–95.9)	88.5 (83.7–93.2)	94.6 (91.8–97.2)
Low-confidence	74.1 (68.4–79.2)	62.4 (52.9–71.8)	81.1 (75.1–87.0)	66.3 (56.8–75.8)	78.3 (72.1–84.4)

CI, confidence interval; NPV, negative predictive value; PPV, positive predictive value.

patterns were uncertain, reviewers had low confidence in their prediction 91.7% of the time.

The impact of discrepancy between the mucosal and vascular patterns was also assessed. In the majority of the cases (81%), both the mucosal and vascular patterns were marked as identical, that is, either both were regular or both were irregular. There was no difference between the choice of vascular and mucosal patterns with regard to the ability to predict the histology of the sample—in 75% and 77% of cases, respectively, the choice led the investigator to make the correct histologic prediction (Table 5).

The overall strength of inter-observer agreement for the prediction of dysplasia in BE using the BING criteria was substantial ($\kappa = 0.681$).

Discussion

BE is thought to progress to EAC via the metaplasia–dysplasia–carcinoma sequence.[33] Careful endoscopic examination of Barrett's epithelium is performed with the goal of early detection of neoplasia.[33] Because NBI provides enhanced endoscopic visualization of the subtle mucosal and vascular changes that occur in the progression of BE to cancer, it potentially could be used to predict the underlying histology of BE visualized on endoscopy. Advantages of the use of NBI over standard WLE include enhanced endoscopic detection of dysplasia in BE, obtaining target biopsies and the necessity of potentially fewer biopsies to establish a diagnosis of BE.[34,35]

Several different classification systems for the prediction of histopathology based on surface patterns in Barrett's epithelium observed with NBI have been proposed.[18–20,23,24] Goda et al[22] developed a complex NBI classification scheme that sought to distinguish specialized intestinal metaplasia from columnar-lined esophagus in BE. Kara et al[19] designed a NBI classification system based on regular vs irregular mucosal and vascular patterns, and normal vs abnormal blood vessels. This system, known as the Amsterdam classification, yielded a relatively high diagnostic value for high-grade intraepithelial neoplasia (sensitivity, 94%; specificity, 76%; positive predictive value, 64%; and negative predictive value, 98%). Sensitivity and specificity were higher in a study of the Kansas classification, criteria developed by Sharma et al[18] comprising 3 distinct mucosal and 2 distinct vascular patterns for the classification of BE dysplasia and cancer. The Kansas classification was used to predict the presence of intestinal metaplasia and HGD with a sensitivity and specificity of 93.5% and 86.7%, and 100% and 98.7%, respectively. Two studies analyzed the accuracy of NBI in the differentiation of dysplasia in BE.[30,31] A systematic review by Curvers et al[31] designed to assess the ability of NBI to differentiate gastric from intestinal type mucosa reported sensitivities ranging from 77% to 100%, specificities of 79% to 94%, and overall accuracies of 88% to 96%, based on data from 8 studies. To further investigate the use of NBI in the differentiation of neoplasia in BE, several analyses of inter-observer agreement have been performed.[25–29] The results of these studies, however, have been disappointing, with moderate to fair inter-observer agreement, and no significant differences in diagnostic accuracy or agreement between experienced and inexperienced assessors.

To date, the various published NBI classification systems are complex, studies of dysplasia prediction have been variable, and inter-observer agreement of these systems have yielded disappointing results. Additionally, previous

Table 5. Accuracy for Predicting of Dysplasia Using BING Criteria

	n (%)	Accuracy, % (95% CI)	Sensitivity % (95% CI)	Specificity % (95% CI)	% High confidence
If mucosal and vascular pattern graded similarly (ie, both either regular or irregular)	582 (80.8)	87.5 (84.5–90)	82.43 (77.43–87.44)	90.56 (87.53–93.58)	70.3
If mucosal and vascular pattern graded different (ie, one regular and other irregular)	78 (10.8)	75.6 (64.6–84.7)	84.85 (72.62–97.08)	68.89 (55.36–82.42)	65.4
If either pattern graded as "uncertain"	60 (8.3)	78.3 (65.8–87.9)	40 (15.21–64.79)	91.11 (82.8–99.43)	76.7

CI, confidence interval.

classification criteria have been based on single-center studies with limited numbers of patients, and were not internally validated.[18–20,24] These factors have limited the use of these classification systems in routine clinical practice. In an attempt to address these shortcomings, our group developed a new, international, prospective, consensus-driven, internally validated NBI classification system. This new classification system, the BING criteria, can be used to predict the presence or absence of dysplasia in BE based on the simple classification of mucosal and vascular patterns as regular (nondysplastic) or irregular (dysplastic). High-confidence predictions by the experts yielded high accuracy, sensitivity, and specificity (92%, 91%, and 93%, respectively). The improvement shown in the diagnostic characteristics from phase 3 and phase 4 probably reflects a small learning curve associated with these criteria. The overall strength of inter-observer agreement of the BING Criteria was substantial, with a κ value of 0.681, an improvement on NBI classification systems reported previously.

Limitations of our study include the use of still images in a web-based survey. Although the use of still images can limit the ability of the reviewer to compare areas of suspicion with surrounding normal mucosa, the web-based survey design is an artificial situation that does not replicate either video-based assessment or real-time endoscopy performed in clinical practice. In addition, images from LGD areas were not included in the study, as there remains a very high inter-observer variability in the diagnosis of this condition. Further study will reveal whether the accuracy and inter-observer agreement of the BING Criteria can be replicated during real-time endoscopy in a clinical setting. Additionally, our analysis was performed using a per-area/location/image design, as opposed to a per-patient basis. An assessment of inter-observer variability in a patient-based analysis (ie, 1 image from 1 patient) would more closely correspond to clinical practice and needs to be tested further. Our aim was to evaluate the first step: develop, validate, and test the criteria. The issue of including LGD was discussed by the investigators before study initiation. However, the surface changes seen on NBI in patients with LGD are not different than that of NDBE, that is, patterns are similar in LGD and NDBE patients. It is possible that the surface changes of LGD cannot be detected by broad surface imaging techniques, such as NBI, but could perhaps by microscopic techniques, such as confocal laser endomicroscopy. Finally, the BING Classification will need to be tested in trainees and practitioners with various levels of experience in different settings (academic vs community).

In summary, we propose a new, consensus-driven, internally validated classification system, the BING Criteria, that can be used to predict the presence or absence of dysplasia in NBI images of BE with a high level of accuracy and substantial inter-observer agreement. The BING Criteria offer endoscopists a simple, user-friendly NBI classification system, with the potential for use in BE surveillance in routine clinical practice.

References

1. Theisen J, Stein HJ, Dittler HJ, et al. Preoperative chemotherapy unmasks underlying Barrett's mucosa in patients with adenocarcinoma of the distal esophagus. Surg Endosc 2002;16:671–673.
2. Sharma P. Clinical practice. Barrett's esophagus. N Engl J Med 2009;361:2548–2556.
3. Pohl H, Welch HG. The role of overdiagnosis and reclassification in the marked increase of esophageal adenocarcinoma incidence. J Natl Cancer Inst 2005; 97:142–146.
4. Lagergren J, Bergstrom R, Lindgren A, et al. Symptomatic gastroesophageal reflux as a risk factor for esophageal adenocarcinoma. N Engl J Med 1999;340: 825–831.
5. Eloubeidi MA, Mason AC, Desmond RA, et al. Temporal trends (1973-1997) in survival of patients with esophageal adenocarcinoma in the United States: a glimmer of hope? Am J Gastroenterol 2003;98:1627–1633.
6. American Gastroenterological Association, Spechler SJ, Sharma P, et al. American Gastroenterological Association medical position statement on the management of Barrett's esophagus. Gastroenterology 2011;140: 1084–1091.
7. Sharma P, Dent J, Armstrong D, et al. The development and validation of an endoscopic grading system for Barrett's esophagus: the Prague C & M criteria. Gastroenterology 2006;131:1392–1399.
8. Wang KK, Sampliner RE. Updated guidelines 2008 for the diagnosis, surveillance and therapy of Barrett's esophagus. Am J Gastroenterol 2008;103:788–797.
9. Levine DS, Blount PL, Rudolph RE, et al. Safety of a systematic endoscopic biopsy protocol in patients with Barrett's esophagus. Am J Gastroenterol 2000; 95:1152–1157.
10. Fitzgerald RC, Saeed IT, Khoo D, et al. Rigorous surveillance protocol increases detection of curable cancers associated with Barrett's esophagus. Dig Dis Sci 2001; 46:1892–1898.
11. Sharma P, McQuaid K, Dent J, et al. A critical review of the diagnosis and management of Barrett's esophagus: the AGA Chicago Workshop. Gastroenterology 2004; 127:310–330.
12. Cameron AJ, Carpenter HA. Barrett's esophagus, high-grade dysplasia, and early adenocarcinoma: a pathological study. Am J Gastroenterol 1997;92: 586–591.
13. Chatelain D, Flejou JF. High-grade dysplasia and superficial adenocarcinoma in Barrett's esophagus: histological mapping and expression of p53, p21 and Bcl-2 oncoproteins. Virchows Arch 2003;442:18–24.
14. Montgomery E, Bronner MP, Goldblum JR, et al. Reproducibility of the diagnosis of dysplasia in Barrett esophagus: a reaffirmation. Hum Pathol 2001;32: 368–378.
15. Kara MA, Bergman JJ. Autofluorescence imaging and narrow-band imaging for the detection of early neoplasia in patients with Barrett's esophagus. Endoscopy 2006; 38:627–631.

16. Gono K, Obi T, Yamaguchi M, et al. Appearance of enhanced tissue features in narrow-band endoscopic imaging. J Biomed Opt 2004;9:568–577.
17. Kuznetsov K, Lambert R, Rey JF. Narrow-band imaging: potential and limitations. Endoscopy 2006;38:76–81.
18. Sharma P, Bansal A, Mathur S, et al. The utility of a novel narrow band imaging endoscopy system in patients with Barrett's esophagus. Gastrointest Endosc 2006;64:167–175.
19. Kara MA, Ennahachi M, Fockens P, et al. Detection and classification of the mucosal and vascular patterns (mucosal morphology) in Barrett's esophagus by using narrow band imaging. Gastrointest Endosc 2006;64:155–166.
20. Singh R, Anagnostopoulos GK, Yao K, et al. Narrow-band imaging with magnification in Barrett's esophagus: validation of a simplified grading system of mucosal morphology patterns against histology. Endoscopy 2008;40:457–463.
21. Hamamoto Y, Endo T, Nosho K, et al. Usefulness of narrow-band imaging endoscopy for diagnosis of Barrett's esophagus. J Gastroenterol 2004;39:14–20.
22. Goda K, Tajiri H, Ikegami M, et al. Usefulness of magnifying endoscopy with narrow band imaging for the detection of specialized intestinal metaplasia in columnar-lined esophagus and Barrett's adenocarcinoma. Gastrointest Endosc 2007;65:36–46.
23. Anagnostopoulos GK, Yao K, Kaye P, et al. Novel endoscopic observation in Barrett's oesophagus using high resolution magnification endoscopy and narrow band imaging. Aliment Pharmacol Ther 2007;26:501–507.
24. Alvarez Herrero L, Curvers WL, Bansal A, et al. Zooming in on Barrett oesophagus using narrow-band imaging: an international observer agreement study. Eur J Gastroenterol Hepatol 2009;21:1068–1075.
25. Singh M, Bansal A, Curvers WL, et al. Observer agreement in the assessment of narrowband imaging system surface patterns in Barrett's esophagus: a multicenter study. Endoscopy 2011;43:745–751.
26. Silva FB, Dinis-Ribeiro M, Vieth M, et al. Endoscopic assessment and grading of Barrett's esophagus using magnification endoscopy and narrow-band imaging: accuracy and interobserver agreement of different classification systems (with videos). Gastrointest Endosc 2011;73:7–14.
27. Curvers WL, Bohmer CJ, Mallant-Hent RC, et al. Mucosal morphology in Barrett's esophagus: interobserver agreement and role of narrow band imaging. Endoscopy 2008;40:799–805.
28. Curvers W, Baak L, Kiesslich R, et al. Chromoendoscopy and narrow-band imaging compared with high-resolution magnification endoscopy in Barrett's esophagus. Gastroenterology 2008;134:670–679.
29. Baldaque-Silva F, Marques M, Lunet N, et al. Endoscopic assessment and grading of Barrett's esophagus using magnification endoscopy and narrow band imaging: impact of structured learning and experience on the accuracy of the Amsterdam classification system. Scand J Gastroenterol 2013;48:160–167.
30. Mannath J, Subramanian V, Hawkey CJ, et al. Narrow band imaging for characterization of high grade dysplasia and specialized intestinal metaplasia in Barrett's esophagus: a meta-analysis. Endoscopy 2010;42:351–359.
31. Curvers WL, van den Broek FJ, Reitsma JB, et al. Systematic review of narrow-band imaging for the detection and differentiation of abnormalities in the esophagus and stomach (with video). Gastrointest Endosc 2009;69:307–317.
32. Landis JR, Koch GG. The measurement of observer agreement for categorical data. Biometrics 1977;33:159–174.
33. Anaparthy R, Sharma P. Progression of Barrett oesophagus: role of endoscopic and histological predictors. Nat Rev Gastroenterol Hepatol 2014;11:525–534.
34. Wolfsen HC, Crook JE, Krishna M, et al. Prospective, controlled tandem endoscopy study of narrow band imaging for dysplasia detection in Barrett's Esophagus. Gastroenterology 2008;135:24–31.
35. Sharma P, Hawes RH, Bansal A, et al. Standard endoscopy with random biopsies versus narrow band imaging targeted biopsies in Barrett's oesophagus: a prospective, international, randomised controlled trial. Gut 2013;62:15–21.

Received July 17, 2015. Accepted November 16, 2015.

Reprint requests
Address requests for reprints to: Prateek Sharma, MD, Department of Gastroenterology (111), Department of Veterans Affairs Medical Center, 4801 E. Linwood Boulevard, Kansas City, Missouri 64128-2295. e-mail: psharma@kumc.edu; fax: (816) 922-4692.

Conflicts of interest
These authors disclose the following: Prateek Sharma: grant support from Olympus, Effexus Pharmaceuticals, Cosmo Pharmaceuticals, CDx Diagnostics. Jacques Bergman: Olympus. Mototsugu Kato: Has served in speaking and teaching commitments for Eisai Co., Ltd., Daiichi Sankyo Company, Ltd., and AstraZeneca K.K. and has received scholarship grants from Eisai Co., Ltd., Takeda Pharmaceutical Co., Ltd., Daiichi Sankyo Company, Ltd., AstraZeneca K.K., and Astellas Pharma Inc. Helmut Messmann: Olympus, Covidien, Norgine, Abbott. Neil Gupta: Research support from Cook Medical, CDx Diagnostics, and Cosmo Pharmaceuticals. Vani Konda: Olympus, Mauna Kea Technologies. Irving Waxman: Olympus, Cook Medical. The remaining authors disclose no conflicts.

Funding
This study was supported by Olympus Inc., Tokyo, Japan.